Available online at www.sciencedirect.com

ScienceDirect

Procedia IUTAM 2 (2011) 35–57

Procedia IUTAM

www.elsevier.com/locate/procedia

2011 Symposium on Human Body Dynamics

Simulation of fatigue-initiated subacromial impingement: clarifying mechanisms

Clark R. Dickerson*, Jaclyn N. Chopp, Stephanie P. Borgs

Department of Kinesiology, University of Waterloo, 200 University Ave W., Waterloo, Ontario, N2L 3G1, CANADA

Abstract

Subacromial impingement in the shoulder precedes many cases of rotator cuff pathology. However, debate exists regarding the mechanism, and even existence, of fatigue-initiated impingement. The controversy centers on two primary impingement mechanisms: 1) superior humeral head migration and 2) scapular reorientation. A linked series of in vivo experiments and in silica simulations accomplishes the integration of stochastic, orthopedic, geometric, kinematic, physiologic, literature-derived, and experimental data sources to help resolve the mechanism debate. A major focus is the multi-scale modeling of relevant variability. The described techniques have direct implications for musculoskeletal modeling and simulation of the shoulder region, with specific application to assessing occupational and activities of daily living in diverse populations.

Peer-review under responsibility of John McPhee and József Kövecses

Keywords: shoulder mechanics; stochastics; kinematics; variability; impingement

1. Introduction

The purpose of this paper is to communicate a framework for a stochastic ‘supermodel’ for population predictions of subacromial impingement. This involves multiple considerations that will be pursued in the introduction, including:

- The motivation behind understanding and preventing shoulder disability
- Clinical and practical definitions of subacromial impingement
- Fundamental aspects of shoulder mechanics and musculoskeletal geometry
- The scope of presently available shoulder orthopaedic geometric models
- The need for variation accountability in subacromial impingement prediction
- The novelty and basis for a stochastic model of subacromial impingement.

* Corresponding author. Tel.: +1-519-888-4567, ext. 37844; fax: +1-519-746-6776.
E-mail address: cdickers@uwaterloo.ca.

2210-9838 © 2011 Published by Elsevier Ltd. Open access under CC BY-NC-ND license.
doi:10.1016/j.piutam.2011.04.005

1.1. The financial and societal burdens of shoulder disability

Shoulder injuries are common, both occupationally and in the population as a whole. These injuries generate considerable financial and social costs internationally, accounting for 13.3% of missed work day cases and 24.7% of missed work days due to musculoskeletal disorders in the United States [1]. High costs of nearly $9,500 CAD in long term disability benefit costs per lost time injury accompany shoulder injuries [2]. This does not include direct health costs, estimated to be approximately $20,000 USD per rotator cuff injury [3] as early as 2003, or other additional indirect costs. In one study, over 34% of shoulder injuries led to more than 30 days off work, compared to 27.7% for wrist and 18.6% for back [4], and median missed days of work due to injury is tripled for shoulder injuries compared to spinal injuries. Additionally, many shoulder injuries have high recurrence rates, such as from 52-90% for anterior dislocation [5-6]. This further exacerbating the level of societal disability associated with shoulder injuries. This combination motivates reduction of shoulder pathologies, most obviously those in the workplace.

1.2. Fundamental aspects of human shoulder mechanics

The human shoulder allows braced placement of the hand and fingers in a wide array of locations and orientations that are necessary to generate forces to perform a spectrum of physical activities. The intricate shoulder morphology, including the gliding scapulothoracic interface, enables this kinematic versatility. However, this high postural flexibility comes at the cost of intrinsic joint stability, as is widely reported [7]. Indeed, the shallowness of the glenoid fossa, critical for the large range of motion, requires stabilization from one or more mechanisms, including active muscle coordination, elastic ligament tension, labrum deformation, joint suction, adhesion/cohesion, articular version, proprioception, and negative internal joint pressure [8-9]. Beyond this issue, there are further complications, including the kinematic redundancy of the shoulder girdle (known as the shoulder rhythm), and musculoskeletal mechanical indeterminacy, as there are far more actuators (muscles) than there are degrees of freedom (DOF) in the system. Finally, interactions of the many components of the shoulder mechanism are also critical to fully model the system.

1.3. Theories and evidence for fatigue-induced subacromial impingement initiation

Maintaining the subacromial space is critical to rotator cuff health. The subacromial space is situated inferior to the acromion of the scapula and superior to the superior aspect of the proximal humerus, in the proximity but superior to the glenohumeral joint. Importantly, the supraspinatus and biceps tendons and the shoulder bursa occupy part of this space. Subacromial impingement (SAI) typically precedes rotator cuff disease, and exists when this space is decreased and interposed tissues are compressed. Of particular concern is the supraspinatus tendon, which is generally the site of initial rotator cuff pathologies [10]. Two mechanistic fatigue-related SAI initiation theories dominate academic discussion [11] superior humeral translation and scapular dyskinesis. The relative contributions of these mechanisms to SAI genesis are uncertain. *Superior humeral translation:* This theory supposes that translation of the humeral head decreases the subacromial space. If the rotator cuff, despite its anatomical positioning to provide joint stabilizing forces, cannot maintain compression of the humeral head in the glenoid cavity due to dysfunction, the head translates superiorly. Several studies have confirmed this translation occurs with muscle fatigue [12-15]. *Scapular dyskinesis:* This theory supposes that weak or dysfunctional muscles (i.e. after fatigue) improperly guide scapular movement, resulting in reduction of the subacromial space. Evidence to support the theory has been mixed, but tends to indicate that impingement is more likely attenuated [16-18] rather than amplified [19] by this mechanism. As discussed in Section 3 of this paper, high variability exists with respect to both of these responses following fatigue.

1.4. Existing biomechanical shoulder analyses

Historically, biomechanical study of shoulder function and injury mechanisms has been limited, partly due to the described complexity of the shoulder girdle movements [20-22] and partly due to a focus on other important health concerns [23]. However, as specific tissue exposures are posited to relate to both the occurrence [24-25]) and aetiology of shoulder diseases and disorders [26], it is imperative to quantify shoulder tissue loads and kinematics reliably. Despite impressive progress along these lines, the determination of these specific values is neither trivial nor fully accomplished for a wide range of relevant activities.

Recently, however, several research groups have generated mathematical models to predict shoulder muscle forces for generic activities [21, 24, 27-37] and these models depend largely on cadaveric geometric data. The empirical evaluation of these models has primarily targeted constrained, planar exertions. However, analyses of most manual activities are complex due to inertial components that alter exposures and viscoelastic tissue responses. This requires models that have been evaluated for a range of conditions, such as ours [31-32].

1.5. The problem with determinism and injury prediction

Unfortunately, most currently described large-scale shoulder muscle force models are deterministic, in that most internal parameters (and thus outputs) are constrained to single values. In a population, however, the factors are inconsistent between and within individuals (depending on the parameter). Therefore deterministic models do not represent many or most possible exposure scenarios in a population. This may lead to systematically inaccurate generalization of the scope of application of findings. A fully stochastic model, conversely, includes modeling of variability in all model stages (inputs/parameters/outputs). In the main body of this paper, four aspects of variability will be focused on: 1) bone morphometry, 2) the shoulder rhythm, 3) fatigue responses, and 4) external physical demands. Variation in all of these parameters can lead to profound differences in outcomes as will be discussed in more detail in Section 3. The common wisdom that ‘the outliers end up in the clinic’ must be applied and distributions, rather than average data, must be assessed for potential injury.

1.6. Theoretical basis and novelty of our approach

The primary novelty of our approach is the consideration of multi-scale variability and its influence on the generation of exposure-induced subacromial impingement. This will be communicated in the framework of considering variability across three classes of data, all of which inform geometric model outputs (Fig. 1):

- External Factors
- Intrinsic Model Factors
- Response Factors

Considering the variability yields output predictions that span the population and by considering variability in external factors, intrinsic model factors, and response factors together, a population predictive model can be generated. This is in sharp contrast to most typically deterministic models.

2. Description of the geometric shoulder model

Several evolutionary publications [31-32, 38-39] document in detail the development and empirical evaluation of the large-scale mathematical biomechanical shoulder model used to conduct this research. The complete model includes three major stages: 1) a geometric reconstruction model representing the bones and muscles of the shoulder, 2) an external dynamic shoulder moment calculation model, and 3) an internal muscle force and tissue load prediction model. Only the first stage, the geometric model, is used in the described research, and thus explanation of the overall model is limited to its description. All

analyses currently performed are with respect to the orthopaedic components which effectively simplifies the model from a musculoskeletal to a skeletal entity. Future investigations will incorporate muscular components as well.

Recreating the geometry of the shoulder mechanism mathematically includes two major conceptual stages: (1) bone parameter definition and (2) shoulder rhythm implementation (including secondary coordinate system definition). The geometric model uses 3-D motion files as input. These files contain either Cartesian coordinates of specific body joint centers and landmarks during a motion or in a pose, defined in a global reference system, or locally defined joint angles. The relevant outputs of the geometric model to the described work are the relative positions and orientations of the humerus and scapula, but their definition is dependent on definition of a torso-based system as well. Initial configuration of the shoulder system is described followed by details of a shoulder rhythm implementation. The stochastic modification of these systems is described in Section 3.

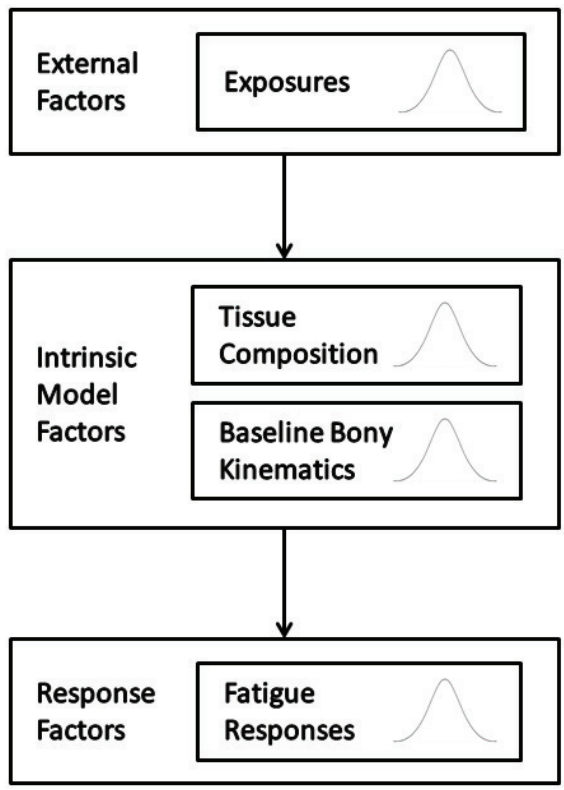

Fig. 1. Simplified flow of information through the geometric model. The four indicated distributional variables are all treated stochastically in the model, yielding a population distribution of model outputs, primarily subacromial space.

2.1. Bone parameter definition

Several descriptions of shoulder musculoskeletal geometric data exist [24, 40-44]. These typically consist of subject-pool mean bony dimensions. The list is limited due to the considerable difficulty in both obtaining and measuring the many components. Although recent attempts to characterize shoulder geometry using less invasive measurements [45-46] have had success, they have been limited to specific muscle analysis. Thus, the cadaveric data sources remain the most completely defined for modeling purposes, particularly of orthopaedic structures. Our definitions rely on these sources.

In our model, five segments describe the shoulder mechanism, similar to a method described by [24]. The segments include of the scapula, the clavicle, the humerus, and the thorax, which includes both the thoracic spine and the ribcage. In addition, a combined radial/ulnar forearm link is included. Joints between most of the segments are treated by default as spherical joints with three degrees of rotational freedom, but no translational degrees of freedom. The exception to this general rotational convention is the elbow joint, which is allowed only one degree of freedom (flexion/extension). Secondarily, translation is allowed at the glenohumeral joint in fatigued conditions in the simulations (Section 3.2).

2.1.1. Segmental coordinate system specification

For the initial simulation model, three of these segments (humerus, scapula and thorax) were described in more detail using 3-dimensional (3-D) vertices data (Fig. 2) from an existing model [31] Vertices data were extracted from NURBS surfaces from the male data of The Visible Human Dataset. The 3-D coordinates of the 1948 and 600 points that constitute the humeral and scapular vertices respectively were located in the scan (NURBS) system. Further, sixteen anatomical landmarks on the humerus, scapula (including five on the glenoid) and torso were visually specified on the NURBS surfaces to create local axis systems (Table 1) coincident with ISB recommendations [47]. Two of these landmarks included the centers of rotation of the humerus (center of the humeral head (CHH)) and scapula (acromioclavicular joint (ACJ)), the local coordinates of which were derived from scan data. Direction cosine matrices were created between the scan system and each of the locally defined axis systems using the generic construction method (Eq. 1):

$$R_{SYS1}^{SYS2} = \begin{bmatrix} C_{11} & C_{12} & C_{31} \\ C_{21} & C_{22} & C_{32} \\ C_{31} & C_{32} & C_{33} \end{bmatrix} \quad (1)$$

Where C_{jk} are the direction cosines or dot products between the scan (k) and local (j) unit vectors (defined in Table 1), and SYS1 is the scan system for these calculations, and SYS2 is alternately the humeral, scapular, sternal, and glenoid systems.

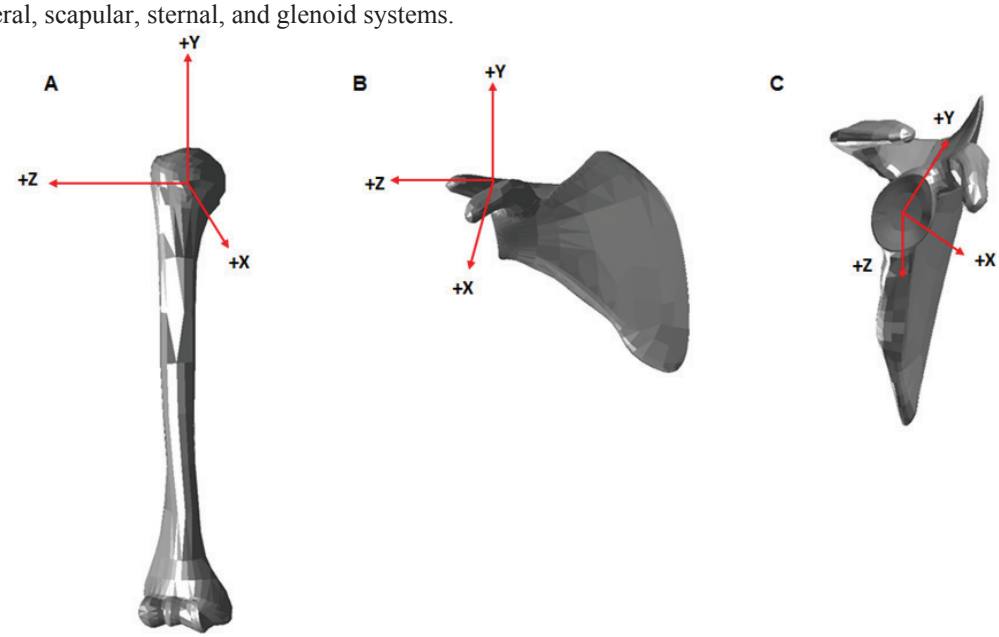

Fig. 2. Local coordinate systems for the segments of the shoulder model. A. Humeral System (+X = Depression (Adduction), +Y = Internal Rotation, +Z = (in the plane of elevation) forward flexion); B. Scapular System (+X = Downward Rotation, +Y = Posterior Tilt, +Z = Protraction). C. Glenoid System (+X = Anterior, +Y = Superior, +Z = Lateral)

Table 1. Definition of local axis systems [47]

Axes	Landmarks Required	Local Coordinate Systems
Scapula	AA = Angulus Acromialis AI = Angulus Inferior TS = Trigonum Scapulae AC = Acromioclavicular Joint	$Z_s = \frac{(AA - TS)}{\lvert(AA - TS)\rvert}$ $temp_s = \frac{(AA - AI)}{\lvert(AA - AI)\rvert}$ $X_s = temp_s \times Z_s$ $Y_s = Z_s \times X_s$
Humerus	CHH = Center of humeral head EL = Lateral Epicondyle EM = Medial Epicondyle $\left[E = \text{Midpoint of Elbow Axis } \frac{(EL + EM)}{2}\right]$	$Y_h = \frac{(GE - E)}{\lvert(GE - E)\rvert}$ $temp_h = \frac{(EM - EL)}{\lvert(EM - EL)\rvert}$ $X_h = temp_h \times Y_h$ $Z_h = X_h \times Y_h$
Thorax	IJ = Incisura Jugularis (suprasternal notch) PX = Processus Xiphoideus C7 = Processus Spinosus of 7th cervical vertebra SC = Sternoclavicular Joint	$Y_t = \frac{(IJ - PX)}{\lvert(IJ - PX)\rvert}$ $temp_t = \frac{(IJ - C7)}{\lvert(IJ - C7)\rvert}$ $Z_t = temp_t \times Y_t$ $X_t = Y_t \times Z_t$
Glenoid	SB = Superior border of glenoid cavity IB = Inferior border of glenoid cavity PB = Posterior border of glenoid cavity AB = Anterior border of glenoid cavity CG = Center of glenoid cavity	$Y_g = \frac{(SB - IB)}{\lvert(SB - IB)\rvert}$ $temp_g = \frac{(AB - PB)}{\lvert(AB - PB)\rvert}$ $Z_g = temp_g \times Y_g$ $X_g = Y_g \times Z_g$

2.1.2. Definition of local position of humeral and scapular vertices

All local vectors to each vertex defined on the humerus (Eq.2) and the scapula (Eq. 3) were calculated for each (i^{th} for humerus; j^{th} for scapula) vertex.

$$\overrightarrow{V_{HUM,\iota}} = R_{SCAN}^{HUM} * \left(\overrightarrow{P_{SCAN,\iota}} - \overrightarrow{0_{SCAN,CHH}}\right) \quad (2)$$

$$\overrightarrow{V_{SCAP,J}} = R_{SCAN}^{SCAP} * \left(\overrightarrow{P_{SCAN,J}} - \overrightarrow{0_{SCAN,AC}}\right) \quad (3)$$

Where $\overrightarrow{V_{HUM,\iota}}$ and $\overrightarrow{V_{SCAP,J}}$ are local vectors describing vertex i for their respective bones, R_{SCAN}^{HUM} and R_{SCAN}^{SCAP} are the respective rotation matrices from the scan to the humeral and scapular systems (derived from Eq. 1), $\overrightarrow{P_{SCAN,\iota}}$ and $\overrightarrow{P_{SCAN,\iota}}$ are the scan system positions of vertex i or j, and $\overrightarrow{0_{SCAN,CHH}}$ and $\overrightarrow{0_{SCAN,AC}}$ are the scan system positions of the origins of the local humeral and scapular systems.

2.1.3. Setting the Initial (Zero Thoracohumeral Elevation) Position

The humerus and the scapula were initially rotated to be oriented according to the mean neutral postures recorded previously (Tables 2 and 3). As the orthopedic orientation data was presented in terms of Euler rotations from a torso-based coordinate system, rotation matrices for the humerus and scapula in

the torso system were derived from measured Euler angles using Eq. 4 and Eq. 5, which are derived from YX'Y'' and XY'Z'' Euler sequences, respectively (Wu et al., 2005).

$$R_{TOR}^{HUM} = \begin{bmatrix} c\psi_h \cdot c\alpha_h - c\beta_h \cdot s\psi_h \cdot s\alpha_h & s\psi_h \cdot s\beta_h & c\psi_h \cdot s\alpha_h + c\alpha_h \cdot c\beta_h \cdot s\psi_h \\ s\alpha_h \cdot s\beta_h & c\beta_h & -c\alpha_h \cdot s\beta_h \\ -c\alpha_h \cdot s\psi_h - c\psi_h \cdot c\beta_h \cdot s\alpha_h & c\psi_h \cdot s\beta_h & c\psi_h \cdot c\alpha_h \cdot c\beta_h - s\psi_h \cdot s\alpha_h \end{bmatrix} \quad (4)$$

Where R_{TOR}^{HUM} is the rotation matrix from the torso coordinate system to the humeral system, c = cosine, s = sine, α_h = plane of elevation, β_h = humeral elevation, ψ_h = axial rotation

$$R_{TOR}^{SCAP} = \begin{bmatrix} c\psi_s \cdot c\alpha_s - s\psi_s \cdot s\alpha_s \cdot s\beta_s & -c\beta_s \cdot s\psi_s & c\psi_s \cdot s\alpha_s + c\alpha_s \cdot s\psi_s \cdot s\beta_s \\ c\alpha_s \cdot s\psi_s + c\psi_s \cdot s\alpha_s \cdot s\beta_s & c\psi_s \cdot c\beta_s & s\psi_s \cdot s\alpha_s - c\psi_s \cdot c\alpha_s \cdot s\beta_s \\ -c\beta_s \cdot s\alpha_s & s\beta_s & c\alpha_s \cdot c\beta_s \end{bmatrix} \quad (5)$$

Where R_{TOR}^{SCAP} is the rotation matrix from the torso coordinate system to the scapular system, c = cosine, s = sine, α_s = Up/Downward Rotation, β_s = Ant/Posterior Tilt, ψ_s = Pro/Retraction

The initial non-fatigued pose of the humerus was defined as 0° of humeral elevation, 30° plane of elevation and 0° internal/external rotation, rotated about the center of the humeral head with the center of the humeral head located 0.85mm below a centered position relative to the glenoid cavity along the superior/inferior (positive y) glenoid axis per previous empirical data [12]. The neutral non-fatigued position of the scapula was defined as 0.69° of upward rotation, 0.67° of posterior tilt and -1° of retraction, rotated about the acromioclavicular joint (AC), and again was derived from a prior experimental study [16].

2.1.4. Model Manipulation Methodology

In order to represent the desired relative positions and orientations of the humerus and scapula, several computational steps are required, including acromioclavicular joint (ACJ) spatial definition in the torso system and specification of the rotation matrix between the glenoid and scapular systems, R_{GLEN}^{SCAP}, through use of a directional cosine matrix approach (Eq. 1). This allowed deliberate 3-D positioning of the center of the humeral head relative to origin both the glenoid, scapular, and torso systems (Eq. 6 and 7).

$$CHH_{GLEN} = z_{GLEN} * \vartheta_{CHH} + y_{GLEN} * \varphi_{CHH} \quad (6)$$

Where CHH_{GLEN} is the vector describing the center of the humeral head in the glenoid system, z_{GLEN} is the positive glenoid z-axis pointing out of the fossa, ϑ_{CHH} is the offset along the positive glenoid z-axis (3.2cm was used), y_{GLEN} is the positive glenoid y-axis running from inferior to superior on the glenoid face, and φ_{CHH} is the superior migration due to fatigue, with positive values indicating superior and negative values inferior migration.

$$CHH_{TOR} = AC_{TOR} + R_{SCAP}^{TOR} * \overrightarrow{V_{SCAP,\overline{ACCG}}} + R_{SCAP}^{TOR} * R_{GLEN}^{SCAP} * CHH_{GLEN} \quad (7)$$

Where CHH_{TOR} is the position of the center of the humeral head in the torso system, AC_{TOR} is the position of the acromioclavicular joint in the torso system, R_{SCAP}^{TOR} is the rotation matrix from the scapular system to the torso system (the inverse of Eq. 4), and $\overrightarrow{V_{SCAP,\overline{ACCG}}}$ is the vector describing the location of the center of the glenoid in the scapular system.

All local humeral and scapular vertices were then described with respect to a common torso-based system (Eq. 8 and 9):

$$HUM_{TOR,i} = CHH_{TOR} + R_{HUM}^{TOR} * \overrightarrow{V_{HUM,i}} \quad (8)$$

Where $HUM_{TOR,i}$ is the position of the i[th] humeral vertex in the torso system, CHH_{TOR} is the result of Eq. 7, R_{HUM}^{TOR} is the rotation matrix from the humerus system to the torso system (the transpose of Eq. 3), and $\overrightarrow{V_{HUM,i}}$ is the result of Eq. 2.

$$SCAP_{TOR,j} = AC_{TOR} + R_{SCAP}^{TOR} * \overrightarrow{V_{SCAP,J}} \quad (9)$$

Where $SCAP_{TOR,j}$ is the position of the j[th] scapular vertex in the torso system, AC_{TOR} is the position of the acromioclavicular joint in the torso system, R_{SCAP}^{TOR} is the rotation matrix from the scapular system to the torso system (the transpose of Eq. 4), and $\overrightarrow{V_{SCAP,J}}$ is the result of Eq. 2.

It should be noted that because $R_{HUM}^{TOR}$and R_{SCAP}^{TOR} are the transposes of Eq. 3 and Eq. 4, respectively, they are directly influenced by the specified Euler Angles for the humerus and scapula for all model simulations.

2.1.5. Extracting subacromial space widths from the simulation model

Once bones are positioned for a given simulation the minimum subacromial space width was determined using Eq. 10. The minimum subacromial space width for each simulation was then scaled to anthropometric data [48] and expressed in millimeters. The scaling factor was 1 scan unit = 3.13mm.

$$for\ i = all\ humeral\ points\ \&\ j = all\ scapular\ points:$$
$$SSW = min\left(HUM_{TOR,i} - SCAP_{TOR,j}\right) \quad (10)$$

Where SSW is the minimum acromiohumeral distance, $HUM_{TOR,i}$ is the position of humeral vertex i in the torso system, and $SCAP_{TOR,j}$ is the position of humeral vertex j in the torso system.

2.2. Implementation of a modified shoulder rhythm

It has been well documented that a relationship exists between the positions of the scapula, humerus, clavicle and torso in the human body, and this relationship has been termed the 'shoulder rhythm' [49-51]. One shoulder rhythm implementation designed for the described segmental coordinate systems has been reported in the literature [36]. It was numerically extrapolated from previous reported rhythms [27, 52]. The model is predicated on the consistent relationship of relative movement between the humerus and the sternum system, as described by a set of Euler angles. Using knowledge of the Euler angles that describe the relative orientation of the humerus in the torso system, Euler angles for the scapula in that posture are estimable. For the creation of the geometric model, the described shoulder rhythm is implemented with a slight mathematical modification to accommodate minor differences in bony geometry used. It should be noted that due to the different origin of the shoulder rhythm relationships, different local coordinate systems must be defined for its implementation (Section 2.2.1).

The modification is based on physiological considerations. Beyond the original shoulder rhythm, the scapula is constrained to maintain both the inferior and superior angles outside the surface of the ribcage, as defined by a cylindrical surface. This constraint is implemented through modification of the scapular Euler angle predictions sequentially (by a single degree) until a physiologically valid position was found. The modification is necessitated by small variations associated with varying bony parameters in simulations.

2.2.1. Segmental (bone-centric) coordinate system definitions

The geometric model contains six distinct systems, five of which are used to describe individual segment orientations, and one (sternal) that is necessary to facilitate the calculation of the shoulder rhythm (described in 2.2). All defined coordinate systems are orthonormal and right oriented for the right

shoulder. For the shoulder rhythm, the focus is on the humeral, scapular, and sternal systems (Fig. 3), as these are relevant in its definitions. Further details of the other systems, specifically the clavicle, torso, and forearm, are available in previous manuscripts [31, 53].

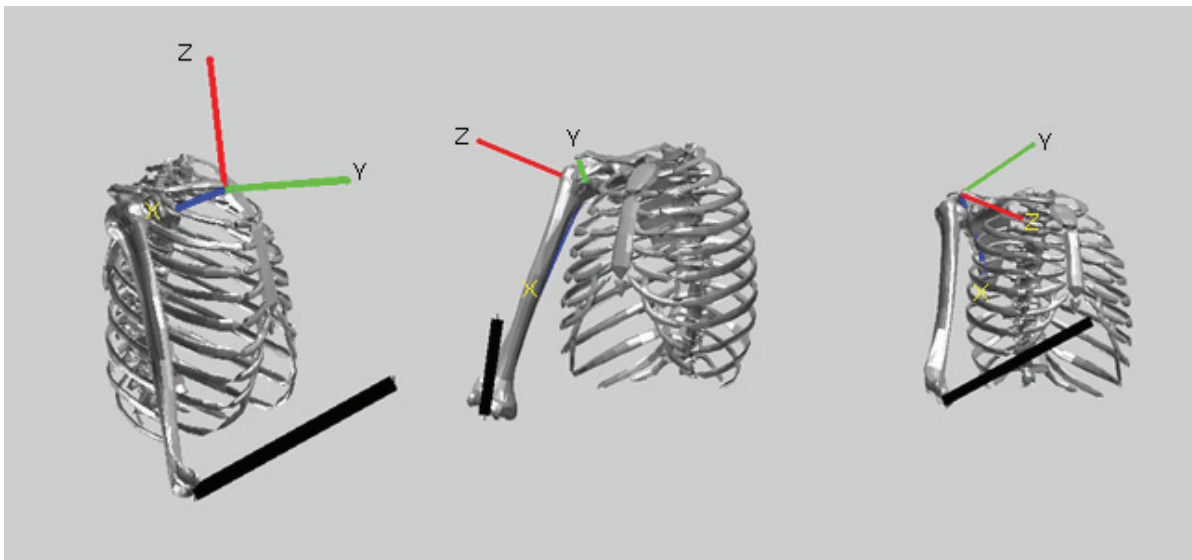

Fig. 3. Local coordinate systems for the segments of the shoulder model. A. sternal system, B. humeral system, C. scapular system

The sternum system is created using three thorax-located landmarks: the superior surface of the first thoracic vertebra, the inferior surface of the twelfth thoracic vertebra, and the right sternoclavicular joint (SCJ). The origin of this system is the right SCJ. The x-y plane is oriented horizontal relative to the torso, with the positive y-axis directed anteriorly, the positive x-axis directed laterally to the right, and the positive z-axis directed cranially.

The scapula system has its origin at the acriomoclavicular (ACJ), and is created using three bone-fixed points, along with the ACJ position. The positive x-axis was directed from the ACJ to the inferior angle of the scapula. The x-y plane contains the superior angle in its first quadrant, resulting in the positive y-axis pointing in a similar direction as the scapular spine. The positive z-axis is the cross product of these two axes, and has a mostly anterior direction, depending on the placement of the scapula on the ribcage for a given posture.

The humeral system has its origin at the center of the humeral head (CHH). This location is derived using the geometric scan data. The positive x-axis is directed through the elbow joint center (EJC). The positive z-axis is directed along the lateral cross product of the long axes of the forearm and humeral segments. The positive y-axis is the cross product of these two axes.

2.2.2. Definition of Euler angles for the initial rhythm

In our model, a (3, -2, 1) set of Euler angles was implemented. These angles are defined:
α = rotation about the sternum positive z-axis (vertical)
β = rotation about the intermediate negative y-axis
δ = rotation about the secondary positive x-axis
The original form of the scapulothoracic rhythm follows (Eq. 10):

$$\begin{aligned}\alpha_s &= 200 + 20 * \cos[0.75 * (\beta_h + 90)] \\ \beta_s &= -87 + 42 * \cos[-0.75 * \beta_h - 70] * (0.1 * \gamma_h / 90 + 1) \\ \gamma_s &= 82 + 8 * \cos\{(\alpha_h + 10) * \sin[0.75 * (\beta_h + 90)]\}\end{aligned} \quad (11)$$

(Subscripts refer to the segment for each angle: h = humerus; s = scapula)

3. Basis for stochastically representing model elements

Biomechanical variability is pandemic in the human population. Anthropometrics as a field is devoted to the study and resolution of differences in the measurable parameters of bodies and their parts [54]. Variability in musculoskeletal tissue characteristics and local joint kinematics is as common as it is in external anthropometrics, and the purpose of this section is to detail some of the reported variability in the musculoskeletal elements of the shoulder region and the importance of this variability with respect to subacromial impingement.

3.1. Exposure Levels

One consideration in the initiation of fatigue related subacromial impingement is the nature of the mechanical exposure the shoulder experiences, which is classically defined in terms of force, body posture, and time–series (i.e. frequency and duration) associated with an exertion. Recent and historic findings emphasize both the level of variability in muscular response to exposures in a population. These were found for similar normalized exposures throughout the body, including at the elbow [55] and shoulder [32] in our own laboratory. Muscle demand is intimately associated with peripheral fatigue, and thus the range of responses to varying loads is essential to capture. The issue of exposure documentation in ergonomics is pervasive, and several different reporting systems have been developed to account for this variability [56-58]. In terms of impingement genesis, the variable responses (described in Section 3.4) are inestimable. Defining a practically relevant distribution of exposure levels, particularly with changing spatial demands [60] is required for developing meaningful population-based subacromial space fatigue predictions.

3.2. Tissue Composition

It is universally recognized that human bones and body parts are variable in terms of size and shape. This is evidenced by large anthropometric covariance across defined segments in dimensions, mass and inertial properties, and individual tissue morphology. In the context of this work, the bony variability that is most closely theorized to be associated with the development of subacromial impingement centers on the subacromial tissues, the acromion (in particular the inferior aspect), the humeral head (in particular the superior aspect), and the glenoid, which contribute to different mechanisms leading to alterations in glenohumeral mechanics.

3.2.1. Subacromial tissues

Recognition of the geometric variability of the soft tissue components across a population is crucial to interpretation of the importance of reductions in the subacromial space. Specific tissues that occupy a portion of this space include the supraspinatus tendon, the subacromial bursa, the long head of the biceps tendon and the shoulder capsule [11, 61-63]. Changes in the morphology of these tissues are best analyzed in the context of available subacromial space, which has received some attention in prior studies. Generally, subacromial space is qualitatively described as having either ‘‘healthy’’ or ‘‘unhealthy’’ magnitude, and is quantified as the 2-dimensional acromio-humeral interval (AHI). Healthy resting range is variously defined as 6-14 mm, and unhealthy resting range below 4-5 mm [64-66]. Thus, an intermediate transitional range with inconsistent characterization exists. Considering this ill-defined transitional range, coupled with excursion measurements taken on such a small scale, a persistent

discrepancy exists regarding the significance of humeral head excursion. It should also be noted that there are substantial changes in the AHI and relative glenohumeral position with arm elevation. Values generally decrease with minimal non-fatigued values occurring near horizontal abduction [67-68], and progressively smaller intervals with elevation in fatigued shoulders [12], with values approaching a mean of approximately 4 mm in some cases.

Having established the normative size of the subacromial space, it is logical to consider the size of the interposed tissues relative to the total space is important in determining how much excursion is associated with tissue impingement and subsequent injury. Girometti et al [69] quantified the morphology of the tissues in the subacromial space in overhead athletes and healthy controls in a neutral posture. The average measurements were 1.43 ± 0.34 mm for bursal and 2.30 ± 0.43 mm for tendon thickness, with a measurement of 8.55 ± 0.85 mm for the overall subacromial space. Thus, in this position, the tissues occupied approximately 44% of the subacromial space. If the same values for tissue thicknesses are considered in other positions (such as 90 degrees of elevation, where the space has been reported as 4.1 ± 2.0mm), the proportion rises to 91%, although different samples were considered. Regardless, these mean values in the healthy case underscore the importance of even minor changes in humeral positioning relative to the subacromial space, changes that are magnified towards the extremes of the distributions.

3.2.2. Acromial morphology

Acromial shape is described as falling into three main types: Type I: flat, Type II: curved, and Type III: hooked, and has been associated with the likelihood of impingement. In fact, acromion shape has been reported as a high internal predictor of impingement and rotator cuff tears in numerous studies [70-73] and acromial enthesophytes have been theorized to cause tendon compression [74-76]. The acromial shapes are distributed throughout the population, with Type II being the most common (~81%), followed by Type III (~14%) and then Type I (~5%), according to recent reports [77] and are typically classified by acromial angle measured using standard techniques [78]. Some disparity, however, exists regarding the age-relatedness of acromial shape with groups alternatively stating an effect exists [79] or is absent [76-77]. Further, downward sloping anterior acromions (Type III) have been observed in as many as 83% of impingement cases [80]. As demonstrated by the considerable changes in penetration of the subacromial space (Fig. 4), a mechanistic relationship with impingement based on acromial morphology is plausible and should be considered in a holistic model.

Fig. 4. Acromial shapes: A) Type I: flat, B) Type II: curved, C) Type III: hooked. Figure adapted from [70]

3.2.3. Humeral head morphology

Descriptions of humeral head morphology center primarily on the articulating surface and its relationship to the glenoid and humeral shaft. High variability in numerous humeral head dimensions, including radius of curvature, diameter, thickness, retroversion, and translational offsets have been reported multiple times [81-83]. The variability can result in substantial changes to both glenohumeral kinematics [84] and consequently reduction of the already very limited subacromial space (discussed previously in Section 3.1.1).

3.2.4. Glenoid morphology

Similarly to humeral head morphology, the glenoid geometric characteristics are highly variable and influential for relative glenohumeral kinematics in both translational and rotational terms. The classification can be made in terms of normal and abnormal categories, with four abnormal subgroups of posterior, superior, global, and anterior erosions [85]. Significant variability is apparent in glenoid morphology in terms of glenoid height, width, version, inclination, and coracoid-glenoid and acromion base-glenoid distances [82, 85-87]. This variability can have important implications for humeral head stabilization [88] and responses (including impingement) to destabilizing events, such as muscle fatigue.

3.3. Shoulder Rhythm

The closed-link shoulder girdle creates the phenomenon known as the shoulder rhythm, or linked movement of the humerus, clavicle, scapula, and thorax. These movements have been studied in detail [52, 89] for routine situations, but not for many other postural configurations. One hallmark of all rhythm studies is that although the rhythm has low intra-subject variability, there is very high inter-subject variability. Differences in glenohumeral relative orientation can substantially influence subacromial space, creating different impingement likelihoods. Respecting this variability, rather than depending on regression-based population guidelines for a common rhythm, is thus important when considering impingement genesis.

3.4. Kinematic Fatigue Responses

Through a series of in vivo experiments, both in our lab as well as those of others, substantial variability in the response to fatiguing exertions has been observed. While in some ways inseparable from the external exposures applied to generate fatigue, the response to similar exposures are highly variable across persons. Two major responses are focused on in this paper: humeral superior migration and scapular orientation changes.

3.4.1. Humeral migration

Research efforts evaluating superior humeral head migration following holistic rotator cuff fatigue have all reported modest mean migration values. These are typically on the order of approximately 1mm; with reported values of 0.98mm [13], 0.79mm [15], 1.22mm [14], and 0.63mm [12]. Common to each study, however, is high inter-subject variability (Fig. 5). Each of these studies with one exception [14] reported a standard deviation ranging from 0.64mm to 2.51mm with a mean of 2.20mm. Chopp et al. [12] measured humeral head migration following a fatiguing protocol that exhausted the rotator cuff. The mean magnitude of migration was 0.63mm; however individual results showed that some participants experienced up to 4.6mm of superior migration. As previously mentioned, a normal healthy AHI is approximately 8.5mm and decreases with arm elevation [61, 67-68]. Further, tissues occupy a mean of 3.7mm (44%) of this space. Thus, even these modest migration values of 1mm can pose risk for impingement. However, the variability in this research becomes very important, as certain individuals, specifically those with migration up to 5mm, will be at an almost sure risk of impingement.

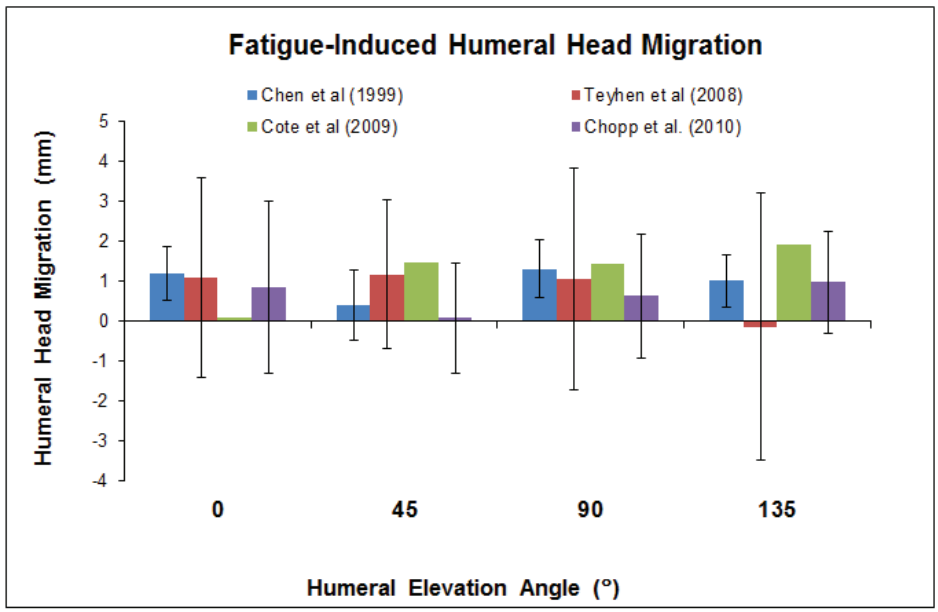

Fig. 5. Fatigue-Induced humeral head migration as reported by multiple literature sources [12]

3.4.2. Scapular Orientation

The orientation of the scapula has been reported to be affected by upper extremity muscle fatigue. The polarity of these changes differs between studies and thus the variability in the literature is high. Downward rotation, anterior tilt and protraction of the scapula are associated with rotator cuff tears and/or clinical impingement [90-92]. However, in the presence of rotator cuff debilitation, by means of fatigue, both these impingement causing orientation changes [19] and conversely impingement-sparing orientation changes exist [16-18]. Despite the polarity of orientation change, each study has reported significant variability indicating that the fatigue-related changes are subject specific. Particularly for protraction/retraction, the variability has been reported to be so high that some subjects displayed impingement sparing following fatigue, and others impingement causing strategies (Fig. 6). Further, aside from the variability between subjects within a study, there has been high variability between studies under similar conditions; thus making inter-study comparisons impossible.

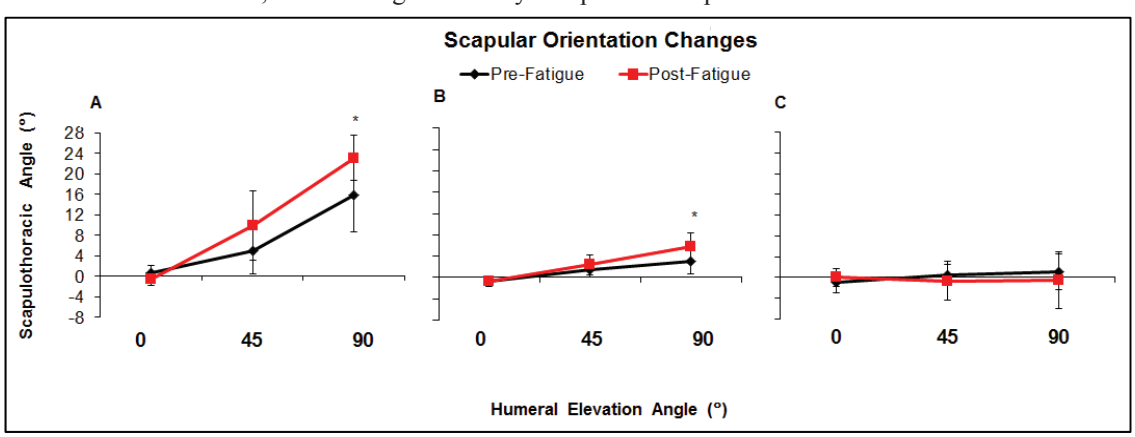

Fig. 6. Effect of fatigue and arm angle on (A) scapular rotation, (B) scapular tilt, and (C) scapular protraction/retraction; Stars (*) letters indicate significant differences between fatigue state ($P<0.05$). Note: Negative values indicate upward rotation, posterior tilt and retraction. Adapted from [16]

4. Incorporating variability – initial efforts for fatigue responses

The three-dimensional orthopaedic model outlined in Section 2.1 was employed to measure the relative contributions of the aforementioned mechanisms to changes in subacromial width and thus the likelihood of fatigue-induced impingement. Empirical data collected from previous research [12, 16] was used to manipulate the orientation of the humerus and scapula relative to the torso (as described in Section 2.1.4) and the corresponding minimum subacromial space width was calculated (as described in Section 2.1.5). Four different conditions were constructed using the humeral head migration (HHM) and scapular orientation (SO) fatigue data [12, 16], which is presented in Tables 2 and 3:

1. Control (Pre-fatigue HHM and SO)
2. Scapular Orientation Only (Pre-fatigue HHM, Post-fatigue SO)
3. Humeral Head Migration Only (Post-fatigue HHM, Pre-fatigue SO)
4. Combined (Post-fatigue HHM and SO)

Further, three different response scenarios were considered:

1. Mean: used mean data for HHM and SO.
2. Best case or "impingement sparing": used data included minimal HHM and maximal scapular upward rotation, posterior tilt and retraction.
3. Worst case or "impingement causing": used data included maximal HHM and maximal scapular downward rotation, anterior tilting and protraction.

These 12 different response-mechanism combinations were evaluated at three humeral elevation angles, to coincide with the available data (0°, 45° and 90°). The resulting subacromial space widths associated with each of the 36 angle-response-mechanism conditions are shown in Table 2.

Table 2. Humeral migration before and after a fatiguing protocol [12]. Mean (Minimum to Maximum) values of the Control (Before fatigue) and Fatigued (After fatigue) for humeral head migration. Data is presented for humeral elevation angles of 0°, 45° and 90° in the scapular plane (30 degrees anterior from the frontal plane). Positive values indicate superior migration.

Humeral Elevation Angle (°)	0	45	90
Control Migration ($\bar{\mu}$, Range, mm)	-0.85 (-3.10 to 3.50)	1.56 (-0.87 to 3.90)	1.48 (-2.30 to 3.80)
Fatigued Migration ($\bar{\mu}$, Range, mm)	0.01 (-3.10 to 2.60)	1.63 (-2.20 to 5.00)	2.10 (0.14 to 5.40)

Table 3. Empirical scapular reorientation [16]. Mean (Minimum to Maximum) values of the Control (Before fatigue) and Fatigued (After fatigue) for rotation, tilt, pro/retraction. Data is presented for humeral elevation angles of (A) 0°, (B) 45° and (C) 90° in the scapular plane (30 degrees anterior from the frontal plane). Positive values indicate upward rotation, posterior tilt, retraction.

(A) 0° Humeral Elevation Angle			
Orientation	Rotation	Tilt	Pro/Retraction
Control Orientation ($\bar{\mu}$, Range, °)	0.82 (-2.18 to 2.89)	0.69 (-0.21 to 2.40)	-1.57 (-3.39 to 1.15)
Fatigued Orientation ($\bar{\mu}$, Range, °)	-1.01 (-2.16 to 0.80)	0.62 (-0.39 to 1.84)	0.06 (-2.23 to 3.18)

(B) 45° Humeral Elevation Angle			
Orientation	Rotation	Tilt	Pro/Retraction
Control Orientation ($\bar{\mu}$, Range, °)	5.34 (-1.73 to 13.24)	-1.84 (-4.87 to -0.15)	0.19 (-2.85 to 2.88)
Fatigued Orientation ($\bar{\mu}$, Range, °)	8.99 (0.67 to 17.91)	-2.53 (-5.13 to -0.35)	-0.12 (-6.09 to 6.64)

(C) 90° Humeral Elevation Angle			
Orientation	Rotation	Tilt	Pro/Retraction
Control Orientation ($\bar{\mu}$, Range, °)	17.14 (4.50 to 25.39)	-3.37 (-7.62 to -0.79)	1.38 (-2.79 to 7.62)
Fatigued Orientation ($\bar{\mu}$, Range, °)	23.17 (18.85 to 31.35)	-5.98 (-11.58 to -2.81)	0.58 (-5.64 to 8.06)

Table 4. The minimum subacromial space width (mm) at humeral elevation angles of 0°, 45° and 90° for each of the four conditions (Control, Scapular Orientation Only, Humeral Head Migration Only, Combined). Results are reported for simulations using mean data, worst case (impingement causing) data and best case (impingement sparing) data.

	Mean (mm)			Impingement Causing (mm)			Impingement Sparing (mm)		
	0°	45°	90°	0°	45°	90°	0°	45°	90°
Control	12.1	7.7	4.5	9.2	5.6	2.8	13.2	10.6	7.4
Scapular Orientation Only	11.7	8.0	5.1	9.1	6.0	1.9	12.9	10.4	8.2
Humeral Head Migration Only	11.9	7.7	3.9	9.9	4.6	2.2	13.2	11.2	5.9
Combined	11.4	7.9	4.5	9.8	5.0	1.5	12.9	11.1	6.8

Humeral head migration was primarily impingement causing and scapular orientation changes were primarily impingement sparing (Table 4), coincident with previous findings [12, 16]. Further, the magnitudes of the subacromial widths reinforce the implications of high inter-subject variability on impingement probability. These implications are most pronounced at 90° of humeral elevation, where subjects experiencing the worst combination of humeral head migration and scapular reorientation had a subacromial space width of 1.5mm, compared to 6.8mm for those experiencing the opposing best impingement sparing scenario. Recalling earlier average tissue widths interposed in the space (Section 3.2.1), it is clear that for some persons the contents of the space may exceed its size following repeated or prolonged exercise that induces general rotator cuff fatigue. Thus, aside from the variability of the inputs themselves (described in Sections 3.4.1 and 3.4.2) there is evidence of variability in their overall contributions to changing subacromial space width. This further reinforces the need to model injury prediction stochastically. This proof-of-concept investigation also motivates our ongoing efforts to more completely consider the multiple sources of variability (Fig. 1) that may influence the incidence of subacromial impingement.

5. Incorporating variability – prospective future implementations

The application of stochastic modeling to shoulder kinematics and biomechanics is in its infancy, but holds substantial potential for insights into population health dysfunction. To enable more meaningful consideration of variability, our research group is engaged in various studies intended to accomplish several major components of building a more population-based probabilistic model:

- Quantify population variability for tissue composition, including bony morphology, soft tissue dimensions, muscle attachment sites, and tissue mechanical capabilities and responses
- Quantify population variability in the healthy shoulder rhythm, including consideration of axial humeral rotation and multiple planes of humeral elevation
- Quantify population variability in response to changing external mechanical demands in terms of their influence on muscular demand and posture
- Quantify population variability in kinematics in the fatigued state

Achieving characterizations of the population distributions of these factors are a necessary first step in the final model construction. In this section further details of representative examples of the pursuit of these distributions are discussed, as well as a conceptual integration of the multiple variability sources into a cohesive, more comprehensive impingement prediction model.

5.1 Quantifying population variability in tissue composition: orthopaedic morphology

Although data sets exist for various musculoskeletal dimensions, capabilities, and configurations, many of the published descriptions are insufficient for detailed subsequent modeling. Our current efforts focus on orthopaedic variability, and thus will be highlighted here.

Representing the variability of morphologic features of bones of the upper extremity will allow for increased model applicability to real-life scenarios. Furthermore, morphologic characteristics of bone can

be used to identify muscle attachment sites, defining the force producing capability of upper extremity muscles. Currently, novel techniques are being implemented to integrate sets of upper extremity bones into the existing kinematic model (described in Section 2). These include advanced image acquisition, processing and identification to define orthopaedic characteristics and muscle attachment sites digitally. Previous attempts were typically done manually, typically with callipers, which introduces the possibility of human error. Small sets of tissue were also typically used due to the labour intensive extraction of musculoskeletal data.

With our approach, images are acquired from sets of human cadaver upper extremity bones. The sets include the upper sternum (including the sternoclavicular articulation); left and right clavicles; left and right scapulae; and left and right humeri. The bones are scanned using a high resolution (StarCam FW-3R 3D White Light Camera (VX Technologies Inc., Alberta, CAN), which produces three-dimensional (3-D) point clouds representing the bone's surface. Multiple point clouds are combinable into watertight objects (Fig. 7) using pattern matching techniques within Geomagic Studio 9 (Geomagic, North Carolina, US). These watertight 3-D bones can then be used to extract precise information about specific morphologic characteristics including acromial shape (Section 3.2.2) and muscle attachment sites. Further, these 3-D representations can be implemented into our geometric model to quantify changes in the width of the subacromial space when different kinematic profiles are introduced.

As previously mentioned, there is variation in bone morphology of the shoulder across populations. Quantifying this variability within cadaver populations is a first step to stochastically representing the observed trends. It is important to incorporate this randomness into model design as it can help with predictions of phenomena as well as definitions of boundary conditions. Furthermore, building into a model stochastic flexibility of inputs and constraints allows it to be applied to large, variable populations such as those encountered in the life sciences.

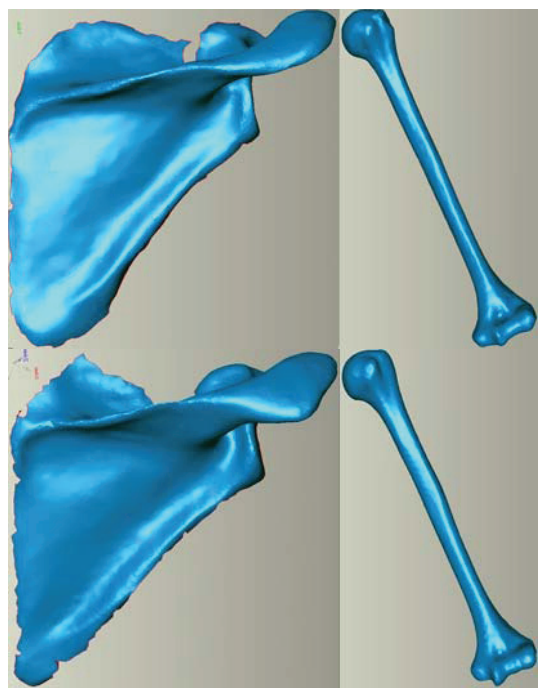

Fig. 7. Visual comparison of sets of scanned shoulder bones. Within each set from left to right are the posterior surface of the scapula and anterior surface of the humerus. Note differences in the bicipital groove and gross scapular spine (and acromial) shape. Both will influence muscle actions.

In addition to this work on characterizing bony morphology, we are also in the process of extracting all relevant morphological distributions to enhance our characterization of population variability, including sources mentioned specifically in section 3.2. Other model factors will also be treated stochastically, as described in Section 5.5.

5.2 Variability in the shoulder rhythm

Changes in shoulder bone orientations alter both relative orthopaedic orientations and muscular lines-of-action, altering the ability of specific muscles to balance external moments. Accurate measurements of bone orientations are thus critical to correctly predict structural loads and subacromial dimensions. Unfortunately, dynamic scapular orientations cannot be externally measured reliably due to the overlying skin displacement with arm movement, despite the attractiveness of comprehensive relative bone orientation data throughout a movement or exertion. Alternatively, mathematical "rhythms", or relative bone orientations, are producible by first measuring the bone orientations at static postures and then fitting equations to predict orientations based on measured arm (humeral) orientations. Prior work has mostly focused on a limited range of arm elevation and excluded extreme overhead postures and humeral axial rotation [52, 89]. Indeed, the current rhythm in our model is derived from data largely extrapolated [36] from measurements for arm elevations up to 90° [52]. We are in the midst of quantifying the shoulder rhythm across the widest range of arm postures ever described for a single population, and are doing so dynamically and statically. This will include the formerly unmeasured influence of axial humeral rotation, and in overhead postures, which are associated with negative physical outcomes [95-96]. Our working hypothesis is that the rhythm is highly dependent on all humeral rotations, and that this will emerge from our modeling procedures. The static and dynamic investigations are described in turn:

Static measures: At the conclusion of the study, scapular orientations will be measured by palpation with a stylus, a scapular locator [97] and an acromial marker cluster [98] for 35 subjects at 42 unique humeral orientations, defined by 3 planes of elevation: 0°, 45°, 90° clockwise from the frontal plane, 5 arm elevations: 0^o, 45^o, 90^o, 135^o, 180^o, and 3 humeral rotations: neutral, and maximal internal and external rotation. Multiple regression analyses of variance (ANOVA)-based models will be used to define rhythm equations that span these novel postures, as well as indicate differences between recording techniques for use in future measurements. Inclusion of the novel rhythms will then improve internal model validity across the range of feasible arm placements, and, in the context of variability, help to define how different the characteristic pattern is across individuals.

Dynamic measures: This investigation will provide a detailed description of normative 3-D dynamic shoulder kinematics in seven vertical planes of thoracohumeral elevation, along with inter-subject variability in these kinematics. This will define the population consistency of shoulder joint rotations. Intra-class correlation coefficients (ICC) (Type 3,1) and standard errors of the mean (SEM) will be used to assess the reliability of trial-to-trial measurements of joint rotations and EMG. 3-way repeated measures ANOVA will be used to test the effects of thoracohumeral elevation plane, elevation angle, and phase (i.e. raising or lowering) on shoulder joint angles. Moreover, these analyses will be used to determine if any changes in kinematics associated with altering the independent variables (i.e. plane, elevation angle, and phase) are larger than the common variability inherent between healthy individuals. The final product will be normative kinematic profiles similar to those produced in gait research [99], which will enable the introduction of variability into dynamic simulations.

5.3 Variability in muscular responses to external physical demands

Another avenue of variability definition being pursued is the influence of manual force requirements on specific and general muscular activation in the shoulder, including the rotator cuff. We have amassed data for 20 subjects performing 570 one-handed manual exertions located at 70 spatial locations, with 5 different force magnitudes and in 6 directions while recording posture and the muscular activations of 14 unilateral electromyographic sites, which has been partially presented previously [60]. From these

11,000+ trials, we have constructed directional prediction equations for muscle demands that are dependent on the magnitude and direction of the force produced, along with the hand spatial location. These are essential to the estimation of muscular activity and therefore fatigue likelihood, even at low levels [100], which is a proposed mechanism of superior humeral head migration [11]. The large distributional data on muscular responses to identical hand force requirements will provide insight into the interactions between persons and their externally generated forces.

5.4 Variability in kinematics of fatigued shoulders

Although data is presented for exposure to exhaustion (Section 4), sub-exhaustive levels of exposures can also lead to potentially injurious changes in subacromial space. We are in the process of launching a series of experiments to evaluate the variability of kinematic changes to different levels of specific exposures.

5.5 Integration into a stochastic 'supermodel' of subacromial impingement

The ultimate purpose of quantifying these multiple aspects of variability relevant to shoulder biomechanics is to transform the use of computational shoulder models from specific scenario testing vehicles to more holistic probabilistic analysis approaches. While this is not the first attempt to incorporate variability in the study of shoulder biomechanics [26, 101-104], the scope of considered variables in the proposed work will provide different insights. This will be accomplished through modeling in the NESSUS software package using a combination of Monte Carlo simulations and response surface modeling. Beyond the geometric properties previously described (Fig. 1), additional characteristics will be incorporated to create a musculoskeletal stochastic model capable of predicting muscle and joint contact forces. Variables to be incorporated are shown in Fig. 8. All require distributional definition prior to incorporation. Several are geometric, but others relate to fundamental aspects of the force distribution problem and other physiological considerations. This conceptual framework increases the feasibility of population-based exposure analyses across a spectrum of outputs.

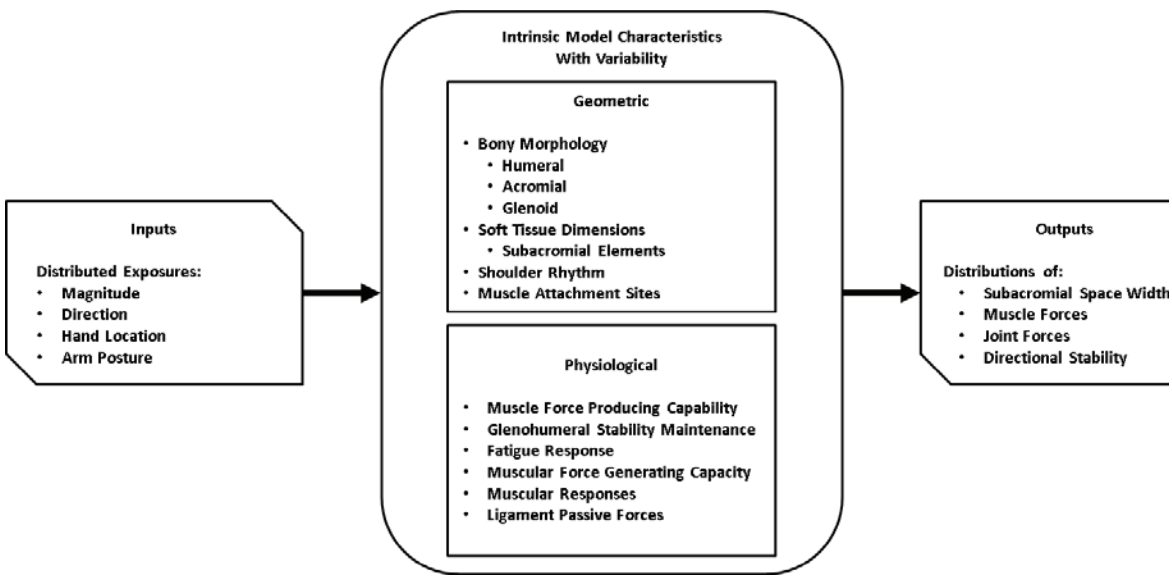

Fig. 8. Musculoskeletal stochastic 'supermodel' including variability in inputs, outputs, and intrinsic model properties. Note that although geometric properties were the focus of this paper, a musculoskeletal approach necessarily also considers physiological variability.

6. Conclusions

The ultimate purpose of the work described in this paper is the more realistic portrayal of population risk of subacromial impingement during exertions common to occupational and daily living tasks. Applications abound throughout the modern world and have profound implications for quality of life, occupational ability or disability, functional independence, and fundamental injury pathways. Specific targeted areas are briefly described below.

6.1 Occupational Tasks

Guidelines for occupational shoulder tasks are largely based on epidemiological data that shows associations without establishing causality. A stochastic model, by considering variability in the population, could help elucidate some of the mechanisms supposed to increase occupational shoulder risk. For instance, working with the arms above shoulder height is known to increase upper extremity muscle demand (including the rotator cuff) which may cause muscle fatigue, as well as pain or discomfort [95-96, 105-108]. It is unclear, however, how intrinsic geometric variability alters the impact of these and many other exposures on health outcomes. Clarifying these mechanisms is critical to developing effective, adopted standard work practices and guidelines.

6.2 Activities of Daily Living

Shoulder dysfunction can lead to the inability to perform even simple daily tasks, and a stochastic model can include the weakest portions of the population for analysis. Individuals with shoulder disorders are known to have increased functional dependency [109] and decreased available shoulder range of motion [110]. Additionally, older persons experience similar reductions in range of motion. Further, symptomatic rotator cuff tear patents have a decreased ability to perform activities of daily living (ADL) [111] which increases the likelihood of requiring long term care. This results in declines in independence and quality of life.

6.3 Summary of Approach

We firmly believe that our approach will progress population modeling of shoulder function and subacromial impingement, while allowing expansion into the study of additional debilitating shoulder health issues, including rotator cuff tears, chronic instability, amongst others. It can help to establish improved work and rehabilitative guidelines, and also to evaluate potential surgical outcomes. The move from determinism to probabilistic thinking is crucial and appropriate given the immensely variable human population of interest, and our overarching purpose is to move towards achieving this conceptual shift and expanding the universality of shoulder biomechanical analyses beyond their current utility.

Acknowledgments

Partial project support came from an NSERC individual discovery grant held by Dr. Clark Dickerson, and from an Early Researcher Award from the Ontario Ministry of Innovation. Equipment used in this experiment was partially funded by the Canada Foundation for Innovation and the Ontario Research Fund. The Workplace Safety and Insurance Board of Ontario Centre for Research Excellence for the Prevention of Musculoskeletal Disorders also funded the humeral migration study that provides data for the described simulation model. Jaclyn Chopp was supported through an NSERC Alexander Graham Bell Fellowship during a portion of the described work.

References

[1] Bureau of Labor Statistics, U.S. Department of Labor. 2009.

[2] Workplace Safety and Insurance Board of Ontario. Musculoskeletal Disorder Report. 2009.

[3] Silverstein B, Kalat J. Washington State Department of Labor. Report TR 40-1-1997 1997.

[4] Washington State Bureau of Labor Statistics Information. 2002.

[5] Rowe CR, Sakellarieds HT. Factors related to recurrences of anterior dislocations of the shoulder. *Clin Orth* 1961;**20**:40-8.

[6] Hovelius L, Augustini BG, Fredin H, Johansson O, Norlin R, Thorling J. Primary Anterior Dislocation of the Shoulder in Young Patients. A Ten-Year Prospective Study. *J Bone Joint Surg* 1996;**78A**:1677-84.

[7] Veeger HE, Van der Helm FC. Shoulder function: the perfect compromise between mobility and stability. *J Biomech* 2007;**40**:2119-29.

[8] Schiffern SC, Rozencwaig R, Antoniou J, Richardson ML, Matsen FA. Anteroposterior centering of the humeral head on the glenoid in vivo. *Am J Sports Med* 2002;**30**:382-7.

[9] Cole BJ, Rodeo SA, O'Brien SJ, Altchek D, Lee D, DiCarlo EF, Potter H, The anatomy and histology of the rotator interval capsule of the shoulder, Clin Orthop Rel Res 2007;**390**:129-37.

[10] Itoi E, Kido T, Sano A, Urayama M, Sato K, Which is more useful, the "full can test" or the "empty can test," in detecting the torn supraspinatus tendon? *Am J Sports Med* 1999;**27**:65-8.

[11] Michener LA, McClure PW, Karduna AR. Anatomical and biomechanical mechanisms of subacromial impingement syndrome. *Clin Biomech* 2003;**18**:369-79.

[12] Chopp JN, O'Neill JM, Hurley K, Dickerson CR. Superior humeral head migration occurs following a protocol designed to fatigue the rotator cuff: A radiographic analysis. *J Shoulder Elbow Surg* 2010;**19**:1137-44.

[13] Chen S K, Simonian PT, Wickiewicz TL, Otis JC, Warren RF. Radiographic evaluation of glenohumeral kinematics: A muscle fatigue model. *J Shoulder Elbow Surg* 1999;**8**:49-52.

[14] Cote MP, Gomlinski G, Tracy H, Mazzocca AD. Radiographic analysis of commonly prescribed scapular exercises. *J Shoulder Elbow Surg* 2009;**18**:311-6.

[15] Teyhen DS, Miller JM, Middag TR, Kane EJ. Rotator cuff fatigue and glenohumeral kinematics in participants without shoulder dysfunction. *J Athl Train* 2008; **43**:352-8.

[16] Chopp JN, Fischer SL, Dickerson CR. The specificity of fatiguing protocols affects scapular orientation: Implications for subacromial impingement. *Clin Biomech* 2011;**26**:40-5.

[17] Ebaugh DD, McClure PW., Karduna AR. Effects of shoulder muscle fatigue caused by repetitive overhead activities on scapulothoracic and glenohumeral kinematics. *J Electromyogr Kinesiol* 2006; **16**:224-35.

[18] McQuade KJ, Dawson J, Smidt GL. Scapulothoracic muscle fatigue associated with alterations in scapulohumeral rhythm kinematics during maximum resistive shoulder elevation. *J Orthop Sports Phys Ther* 1998;**28**:74-80.

[19] Tsai N, McClure PW, Karduna AR. Effects of Muscle Fatigue on 3-Dimensional Scapular Kinematics. *Arch Phys Med Rehabil* 2003;**84**:1000-5.

[20] An KN, Browne AO, Korinek S, Tanaka S, Morrey BF. Three-dimensional kinematics of glenohumeral elevation. *J Ortho Research* 1991;**9**:143-9.

[21] Van der Helm FCT. A finite element musculoskeletal model of the shoulder mechanism. *J Biomech* 1994;**27**(5):551-69.

[22] Van der Helm FCT. Analysis of the kinematic and dynamic behaviour of the shoulder mechanism. *J Biomech* 1994;**27**:527-50.

[23] Rau G, Disselhorst-Klug C, Schmidt R. Movement biomechanics goes upwards: from the leg to the arm. *J Biomech* 2000;**33**:1207-16.

[24] Hogfors C, Sigholm G, Herberts P. Biomechanical model of the human shoulder – I. elements. *J Biomech* 1987;**20**:157-166.

[25] Herberts P, Kadefors R, Hogfors C, Sigholm G. Shoulder pain and heavy manual labour. *Clin Ortho Rel Res* 1984;**191**:166-78.

[26] Hughes RE, An KN. Monte Carlo simulation of a planar shoulder model. *Med & Bio Eng & Comp* 1997;**35**:544-8.

[27] Karlsson D, Peterson B. Towards a model for force predictions in the human shoulder. *J Biomech* 1992;**25**:189-99.

[28] Laursen B, Jensen BR, Nemeth G, Sjogaard G. A model predicting individual shoulder muscle forces based on relationship between electromyographic and 3D external forces in static position. *J Biomech* 1998;**31**:731-9.

[29] Garner BA, Pandy MG. Musculoskeletal model of the upper limb based on the visible human male dataset. *Comp Meth Biomech Biomed Eng* 2001;**4**:93-126.

[30] Holzbaur KRS, Murray WM, Delp SL. A model of the upper extremity for simulating musculoskeletal surgery and analyzing neuromuscular control. *Annals Biomed Eng* 2005; **33**:829-40

[31] Dickerson CR, Chaffin DB, Hughes RE. A mathematical musculoskeletal shoulder model for proactive ergonomic analysis. *Comp Meth in Biomech* 2007;**10**:389-400.

[32] Dickerson CR, Hughes RE, Chaffin DB. Experimental evaluation of a computational shoulder musculoskeletal model. *Clin Biomech* 2008;**23**:886-94.

[33] Dul J. A biomechanical model to quantify shoulder load at the work place. *Clin Biomech* 1988; **3**(3): 124-128.

[34] Charlton IW, Johnson GR. Application of spherical and cylindrical wrapping algorithms in a musculoskeletal model of the upper limb. *J Biomech* 2001;**34**:1209-16.

[35] Favre P, Shekh R, Fucentese SF, Jacob HAC. An algorithm for estimation of shoulder muscle forces for clinical use. *Clin Biomech* 2005;**20**:822-33.

[36] Makhsous M. Improvements, validation and adaptation of a shoulder model. Doctoral Dissertation 1999, Chalmers University, SWE.

[37] Wood JE, Meek SG, Jacobsen SC. Quantification of human shoulder anatomy for prosthetic arm control – II. anatomy matrices. *J Biomech* 1989;**22**:309-25.

[38] Dickerson CR, Martin BJ, Chaffin DB. The relationship between shoulder torques and the perception of muscular effort in loaded reaches. *Ergonomics* 2006;**49**:1036-51.

[39] Gatti CJ, Dickerson CR, Chadwick EK, Mell AG, Hughes RE. Comparison of model-predicted and measured moment arms for the rotator cuff muscles. *Clin Biomech* 2007;**22**:639-44.

[40] Veeger HEJ, Van der Helm FCT, Van der Woude LHV, Pronk GM, Rozendal RH. Inertia and muscle contraction parameters for musculoskeletal modelling of the shoulder mechanism. *J Biomech* 1991;**24**:615-29.

[41] Van der Helm FCT, Veeger HEJ, Pronk GM, Van der Woude LHV, Rozendal RH. Geometry parameters for musculoskeletal modelling of the shoulder system. *J Biomech* 1992;**25**:129-44.

[42] Klein Breteler MD, Spoor CW, Van der Helm FCT. Measuring muscle and joint geometry parameters of a shoulder for modelling purposes. *J Biomech* 1999;**32**:1191-7.

[43] Johnson GR, Spalding D, Nowitzke, Bogduk N. Modelling the muscles of the scapula morphometric and coordinate data and functional implications. *J Biomech* 1996;**29**:1039-51.

[44] Garner Ba, Pandy MG. A kinematic model of the upper limb based on the Visible Human Project (VHP) image dataset. *Comp Meth in Biomech Biomed Eng* 1999;**2**:107-24.

[45] Juul-Kristensen B, Bojsen-Moller F, Ekdahl C. Comparison of muscle sizes and moment arms of two rotator cuff muscle measured by Ultrasonography and Magnetic Resonance Imaging. *Euro J Ultrasound* 2000;**11**:161-73.

[46] Juul-Kristensen B, Bojsen-Moller F, Finsen L, Eriksson J, Johansson G, Stahlberg F, et al. Muscle sizes and moment arms of rotator cuff muscles determined by Magnetic Resonance Imaging. *Cells Tissues Organs* 2000;**167**:214-22.

[47] Wu G, Van der Helm FCT, Veeger HEJ, Makhsous M, Van Roy P, Anglin C, et al. ISB recommendation on definitions of joint coordinate systems of various joints for the reporting of human joint motion - Part II: shoulder, elbow, wrist and hand. *J Biomech* 2005;**38**:981-92.

[48] Frisancho AR, Flegel PN. Elbow breadth as a measure of frame size for US males and females. *Am J of Clin Nut* 1983;**37**:311-4.

[49] Inman VT, Saunders JBCM, Abbott LRC. Observations on the function of the shoulder joint. *J Bone Joint Surg* 1944;**26A**:1-30.

[50] Doody SG, Freedman L, Waterland JC. Shoulder movements during abduction in the scapular plane. *Arch Phys Med Rehabil* 1970;**51**;595-604.

[51] Poppen NK, Walker PS. Normal and abnormal motion of the shoulder. *J Bone & Joint Surg* 1974; **58A**:195-201.

[52] Hogfors C, Peterson B, Sigholm G, Herberts P. Biomechanical model of the human shoulder joint – II. the shoulder rhythm. *J Biomech* 1991;**24**:699-709.

[53] Dickerson CR. A biomechanical analysis of shoulder loading and effort during load transfer tasks. Doctoral Dissertation 2005, University of Michigan, USA.

[54] Chaffin DB, Andersson GBJ, Martin BJ. Occupational Biomechanics. Wiley 2006.

[55] Brookham RL, Middlebrook EE, Grewal T-J, Dickerson CR. The utility of an empirically derived co-activation ratio for muscle force prediction through optimization. *J Biomech* 2011;in press.

[56] Karhu O, Kansi P, Kuorinka I. Correcting working postures in industry: a practical method for analysis. *App Ergo* 1977;**8**(4):199-201.

[58] Matthiassen SE. Diversity and variation in biomechanical exposure: what is it and why would we like to know? *App Ergo* 2006;**37**:419-27.

[59] Jonsson B. The static load component in muscle work. *Eur J App Physio* 1988;**57**:305-10.

[60] Belbeck AL, Chow AY, Dickerson CR. An empirical basis for a spatial shoulder muscle activity map. 33rd Annual Meeting of the American Society of Biomechanics, State College, PA 2009.

[61] Bey MJ, Brock SK, Beierwaltes WN, Zauel R, Kolowich PA., Lock TR. In vivo measurement of subacromial space width during shoulder elevation: Technique and preliminary results in patients following unilateral rotator cuff repair. *Clin Biomech* 2007;**22**:767-73.

[62] Flatow EL, Soslowsky LJ, Ticker JB. Excursion of the rotator cuff under the acromion: Patterns of subacromial contact. *Am J Sports Med* 1994; **22**:779-88.

[63] McFarland EG, Hsu CY, Neira C, O'Neil O. Internal impingement of the shoulder: A clinical and arthroscopic analysis. *J Shoulder Elbow Surg* 1999; **8**:458-60.

[64] Golding FC. The shoulder: the forgotten joint. *Br J Radiol* 1962;**35**:149-58.

[65] Cotton RE, Rideout DF. Tears of the humeral rotator cuff. *J Bone Joint Surg* 1964;**46**B:314-28.

[66] Weiner DS, MacNab I. Superior migration of the humeral head. A radiological aid in the diagnosis of tears of the rotator cuff. *J Bone Joint Surg* 1970;**52B**:524-7.

[67] Graichen H, Bonel H, Stammberger T, Haubner M, Rohrer H, Englmeier KH, et al. Three-dimensional analysis of the width of the subacromial space in healthy subjects and patients with impingement syndrome. *AJR Am J Roentgenol* 1999;**172**:1081-6.

[68] Graichen H, Bonel H, Stammberger T, Englmeier KH, Reiser M, Eckstein F. Subacromial space width changes during abduction and rotational 3-D MR imaging study. *Surg Radiol Anat* 1999;**21**:59-64.

[69] Girometti R, De Candia A, Sbuelz M, Toso F, Zuiana C, Bazzocchi M. Supraspinatus tendon US morphology in basketball players: correlation with main pathologic models of secondary impingement syndrome in young overhead athletes. Preliminary report. *Radiol Med* 2006;**111**:42-52.

[70] Bigliani LU, Ticker JB, Flatow EL, Soslowsky LJ, Mow VC. The relationship of acromial architecture to rotator cuff disease. *Clin Sports Med* 1991;**10**:823-838.

[71] Morrison and Bigliani, Ellman H., Hanker G., Bayer, M. Repair of the rotator cuff end result study of factors affecting reconstruction. *J. Bone Joint Surg* 1986;**70-A**:1136-44.

[72] Worland R.L., Lee D., Orozco C.G., SozaRex F., Keenan J. Correlation of age, acromial morphology, and rotator cuff pathology diagnosed by ultrasound in asymptomatic patients, J Southern Orthopaedic Assoc 1991;**12**:23-8.

[73] Zuckerman JD, Kummer FJ, Cuomo F, Simon J, Rosenblum S, Katz N, The influence of coracoacromial arch anatomy on rotator cuff tears, *J Shoulder Elbow Surg* 1992;**1**:4-14.

[74] Neer CS Anterior acromioplasty for the chronic impingement syndrome in the shoulder. *J Bone Joint Surg* 1972;**54A**:41-50.

[75] Neer CS, Crolg EV, Fukuda H Cuff-tear arthropathy. *J Bone Joint Surg* 1983; **65A**:1232-44

[76] Getz JD, Recht MP, Piraino DW, Schils JP, Latimer BM, Jellema LM, Obuchowski NA. Acromial morphology: relation to sex, age, symmetry and subacromial enthesophytes. *Radiology* 1996;**199**:737-742.

[77] Vaharaki M, Leppilahti J, Hyvonen P, Ristiniemi J, Paivansalo M, Jalovaara. Acromial shape in asymptomatic subjects: a study of 305 shoulders in different age groups. Acta Radiologica 2010;**51**:202-6.

[78] Toivonen DA, Tuite MJ, Orwin JF. Acromial structure and tears of the rotator cuff. *J Shoulder Elbow Surg* 1995;**4**:376–83.

[79] Wang JC, Shapiro MS. Changes in acromial morphology with age, *J Shoulder Elbow Surg* 1997;**6**:55-9.

[80] MacGillivray JD, Fealy S, Potter HG, O'Brien SJ. Multiplanar Analysis of Acromion Morphology. *Am J Sports Med* 1998;**26**:836-40.

[81] Roberts SNJ, Foley APJ, Swallow HM, Wallace WA, Coughlan DP, The geometry of the humeral head and the design of prostheses. *J Bone Joint Surg* 1991;**73B**:647-50.

[82] Iannotti JP, Gabriel JP, Schneck SL, Evans BG, Misra S, The normal glenohumeral relationships. An anatomical study of one hundred and forty shoulders. *J Bone Joint Surg* 1992;**74**A:491-500.

[83] Robertson DD, Yuan J, Bigliani LU, Flatow EL, Yamaguchi K, Three-dimensional analysis of the proximal part of the humerus: relevance to arthroplasty, J Bone Joint Surg 2000;**82A**:1594-1602.

[84] Waturu S, Kazuomi S, Yoshikazu N, Hiroaki I, Takaharu Y, Hideki Y, Acta Orthop. 2005;76:392-6.

[85] Frankle MA, Teramoto A, Luo Z, Levy JC, Pupello D, Glenoid morphology in reverse shoulder arthroplasty: classification and surgical implications. *J Shoulder Elbow Surg* 2009;**18**:874-85.

[86] Churchill RS, Brems JJ, Kotschi H. Glenoid size, inclination, and version: an anatomic study. *J Shoulder Elbow Surg* 2001;**10**:327-32.

[87] von Schroeder HP, Kuiper SD, Botte MJ. Osseous anatomy of the scapula. *Clin Orthop Relat Res* 2001;**10**:131-9.

[88] Sugaya H, Moriishi J, Dohi M, Kon Y, Tsuchiya A. Glenoid rim morphology in recurrent anterior glenohumeral instability. *J Bone Joint Surg* 2003;**85A**:878-84.

[89] deGroot JH, Brand R. A three-dimensional regression model of the shoulder rhythm. *Clin Biomech* 2001; **16**: 735-43.

[90] Endo K, Ikata T, Katoh S, Takeda Y. Radiographic assessment of scapular rotational tilt in chronic shoulder impingement syndrome. *J Orthop Sci* 2001;**6**:3-10.

[91] Lin J, Hanten WP, Olson SL, Roddey TS, Soto-quijano DA, Lim HK, Sherwood AM. Functional activity characteristics of individuals with shoulder dysfunctions. *J Electromyogr Kinesiol* 2005;**15**:576-86.

[92] Ludewig PM, Reynolds JF. The Association of Scapular Kinematics and Glenohumeral Joint Pathologies. *J Orthop Sports Phys Ther* 2009;**39**:90-104.

[94] Chopp JN, Dickerson CR. Resolving the contributions of fatigue-induced humeral migration and scapular reorientation on the subacromial space: An orthopaedic geometric simulation analysis. *Hum Movement Science* 2011 (under review)

[95] Grieve JR, Dickerson CR. Overhead work: Identification of evidence-based exposure guidelines. *Occup Ergon* 2008;**8**:53-66.

[96] Chopp JN, Fischer SL, Dickerson CR. The impact of work configuration, target angle and hand force direction on upper extremity muscle activity during sub-maximal overhead work. *Ergonomics* 2010;**53**:83-91.

[97] Barnett ND, Duncan RDD, Johnson GR. The measurement of three dimensional scapulohumeral kinematics – a study of reliability. *Clin Biomech* 1999;**14**:287-90.

[98] Van Andel C, Van Hutten K, Eversdijk M, Veeger DJ, Harlaar J. Recording scapular motion using an acromion marker cluster. *Gait Posture* 2009;**29**:123-8.

[99] Winter DA. Kinematic and kinetic patterns in human gait: Variability and compensating effects. *Human Movement Science*. 1994;**3**:51-76.

[100] Nussbaum MA, Static and dynamic myoelectric measures of shoulder muscle fatigue during intermittent dynamic exertions of low to moderate intensity. *Eur J App Physiol* 2001;**85**:299-309.

[101] Langenderfer JE, Carpenter JE, Johnson ME, An K-N, Hughes RE. A probabilistic model of glenohumeral external rotation strength for healthy normal and rotator cuff tear cases. *Annals of Biomedical Engineering* 2006;**34**:465-76.

[102] Langenderfer JE, Rullkoetter PJ, Mell AG, Laz PJ. A multi-subject evaluation of uncertainty in anatomical landmark location on shoulder kinematic description. *Computer Methods in Biomechanics and Biomed Engng* 2009;**12**:211-6.

[103] Langenderfer JE, Patthanacharoenphon C, Carpenter JE, Hughes RE. Variability in isometric force and moment generating capacity of glenohumeral external rotator muscles. *Clin Biomech* 2006;**21**:701-9.

[104] Flieg NG, Gatti CJ, Doro LC Langenderfer JE, Carpenter JE, Hughes RE. A stochastic analysis of glenoid inclination angle and superior migration of the humeral head. *Clin Biomech* 2008:**23**:554-61.

[105] Bernard, B. Musculoskeletal Disorders and Workplace Factors. DHHS (NIOSH) Publication No. 97-141. US Department of Health and Human Services, NIOSH, Cincinnati, OH. 1997.

[106] Nussbaum MA, Clark LL, Lanza MA. Fatigue and endurance limits during intermittent overhead work. *American Industrial Hygiene Association Journal* 2001;**62**:446-56.

[107] Punnett L, Fine LJ, Keyserling WM, Herrin GD, Chaffin DB. Shoulder disorders and postural stress in automobile assembly work. *Scandinavian Journal of Work, Environment Health* 2000;**26**:283-91.

[108] Wiker SF, Chaffin DB, Langolf GD. Shoulder posture and localized muscle fatigue and discomfort. *Ergonomics* 1989;**32**: 211-37.

[109] van Schaardenburg, D., Van den Brande, K.J.S, Ligthart, G.J., Breedveld, F.C. & Hazes, J.M.W. (1994) Musculoskeletal disorders and disability in person aged 85 and over: a community survey, *Annals of the Rheumatic Diseases* 1994;**53**:807-11.

[110] Hall LC, Middlebrook EE, Dickerson CR. Analysis of the influence of rotator cuff impingements on upper limb kinematics in an elderly population during activities of daily living. *Clin Biomech* 2011;in press.

[111] Lin, J.C., Weintrub, N. & Aragaki, D.R. (2008) Nonsurgical treatments for rotator cuff injury in the elderly. *J Am Med Directors Association* 2008;**9**:626-32.